2018 IEEE 15th International Symposium on Biomedical Imaging (ISBI 2018)
April 4-7, 2018, Washington, D.C., USA

ACCELERATED HIGH B-VALUE DIFFUSION-WEIGHTED MR IMAGING VIA PHASE-CONSTRAINED LOW-RANK TENSOR MODEL

Lianli Liu[⋆†] *Adam Johansson*[†] *James M.Balter*[†] *Yue Cao*[†] *Jeffrey A.Fessler*[⋆]

[⋆]Department of Electrical Engineering and Computer Science
[†]Department of Radiation Oncology
University of Michigan

ABSTRACT

High b-value Diffusion-weighted MRI (DWI) is promising in cancer imaging but suffers from long acquisition time and low signal-to-noise ratio (SNR). We propose a low-rank tensor model that exploits correlation across both diffusion-induced signal decays and neighboring k-space samples, to accelerate the acquisition of DWI using an extended range of b-values (0 s/mm^2 to 2500 s/mm^2) and limited (orthogonal only) diffusion directions, an imaging scheme that is increasingly used for brain gliomas evaluation. A phase constraint accounts for phase variations between b-values is also applied. Our method integrates parallel imaging and partial Fourier acquisition naturally, and undersamples along phase-encoding direction only. Reconstruction results using both patient and simulated data with an acceleration factor of 8 show improved SNR and reduced aliasing, as compared to parallel imaging only method as well as two other low-rank model-based methods.

Index Terms— cancer imaging, diffusion-weighted imaging, high b-value, constrained reconstruction, low-rank tensor

1. INTRODUCTION

Interest is emerging in acquiring diffusion-weighted magnetic resonance images (DWI) using b-values higher than conventional values (1000 s/mm^2), as it shows potential in better tumor grading and delineation [1–3]. However, the extended sampling of b-values, plus the low signal-to-noise ratio (SNR) and thus the need of repeated acquisition for signal averaging, makes the acquisition time long and inconvenient for clinical use.

Most work in accelerated DWI acquisition focuses on undersmapling the k-q space [4–8], where images are acquired using multiple diffusion directions and two b-values. While in cancer imaging, such as in studies of brain glioma [1–3], usually only 3 orthogonal directions are sampled using a range of b-values. Besides, most existing work uses a moderate b-value at around 1000 s/mm^2, while in high b-value DWI, the extension of b-values to 2000 s/mm^2 and higher, plus the limited sampling of diffusion directions, significantly degrades the SNR and poses challenges for image reconstruction. Although [5] presents reconstruction results using $b = 2000$ s/mm^2 and 64 diffusion directions, that method fails at an acceleration factor of 8 using k-space only undersampling as reported.

Low-rank tensor models have been applied to accelerated MRI and the results are promising [9–12]. However, most methods do not consider the coil dimension, yet multichannel acquisition plays a key role in clinically used acceleration schemes such as parallel imaging. Although [12] builds a tensor of the form space×coil×time and exploits the correlation between coils, acceleration using multi-channel acquisition can use not only the correlation between coils, but also the correlation between neighboring k-space samples. Therefore, exploiting coil correlations only may not fully utilize the benefits of multichannel acquisition. In [13], the author studies tensor models for parallel imaging, but with single image acquisition instead of image series acquisition.

This paper proposes a new low-rank tensor model that exploits both the global low-rank structure of DWI that results from the strong correlation between diffusion signals of voxels and the local low-rank structure that results from the correlation between neighboring k-space samples. The method also includes a phase constraint to account for the large phase variations between b-values and handles partial Fourier acquisition naturally. We evaluate our method using both patient and simulated data and show improved SNR and reduced aliasing, as compared to parallel imaging only method (GRAPPA) [14] and two other low-rank model-based methods [12] and [7].

2. THEORY

2.1. Tensor Construction

In high b-value DWI, a series of 2D DWI images are acquired using N_b different b-values. Each b-value image is acquired using N_c coils. Denote the size of the imaging matrix as $N_x \times N_y$, we record a collection of k-space samples

978-1-5386-3636-7/18/$31.00 ©2018 IEEE

$\mathcal{D} \in \mathbb{C}^{N_x \times N_y \times N_c \times N_b}$.

To model both the local low-rank property, i.e., the correlation between neighboring k-space samples, and the global low-rank property, i.e., the fact that only a few tissue types are present and signal decays among voxels are highly correlated, we first organize k-space samples at each b-value, $\mathcal{D}_b \in \mathbb{C}^{N_x \times N_y \times N_c}, b = 1, 2, \cdots, N_b$ into a block-Hankel matrix $H_b \in \mathbb{C}^{N_c \cdot w^2 \times (N_x - w + 1)(N_y - w + 1)}$ using the SAKE method [15], where w denotes the size of the sliding window that selects a neighborhood of w^2 k-space samples. Next, we stack block-Hankel matrices at different b-values along the third dimension to form a 3D tensor $\mathcal{X} \in \mathbb{C}^{N_c \cdot w^2 \times (N_x - w + 1)(N_y - w + 1) \times N_b}$.

2.2. Phase Variation Correction

One challenge involved in applying low-rank constraint to DWI is the large phase variations across b-values, because DWI sequences are very sensitive to motion. If uncorrected, such phase variations would invalidate the assumption of global low-rankness. Following [7], we estimate the phase map for each coil/b-value from the center of k-space, assuming the phase maps are smooth, and use the estimated phase maps to compensate for phase variations.

Although the phase difference between b-values is due to the motion and should be corrected, the coil phases are important for multichannel acquisition and should be retained.

2.3. Problem Formulation

Based on the low-rank assumptions, we propose the following constrained image reconstruction scheme

$$\begin{aligned} &\hat{\mathbf{y}}, \hat{\mathbf{x}}, \hat{\mathcal{X}} = \arg\min \|\mathbf{d} - \Omega\mathbf{y}\|_2^2 + \lambda \mathbf{R}(\mathcal{X}) \\ &\text{s.t.} \quad \mathbf{y} = \mathcal{F}\mathbf{P}\mathbf{x}, \quad \mathcal{X} = \mathcal{H}\mathcal{F}\mathbf{P_1}\mathbf{x}, \quad \mathbf{x} \in \mathbb{R}^{N_x N_y N_c N_b}, \end{aligned} \tag{1}$$

where $\mathbf{d}$ is the vectorized k-space samples, Ω is the k-space sampling operator, $\mathcal{F}$ is the (full) Fourier transform operator and $\mathcal{H}$ is the operator that constructs block-Hankel matrix as described in [15]. $\mathbf{P} \in \mathbb{C}^{N_x N_y N_c N_b \times N_x N_y N_c N_b}$ is a diagonal matrix that contains the phase information estimated for each coil/b-value image. $\mathbf{P_1}$ is of the same size of $\mathbf{P}$, and is the coil phase information, estimated from the phase maps at $b = 0$ s/mm^2, but replicated N_b times. By forcing $\mathbf{x}$ to be real, we enforce the consistency between the phase information of reconstructed images and the phase estimation using the center of k-space, which makes our algorithm compatible with partial Fourier acquisition [16].

To enforce the low-rank structure, we choose the regularizor $\mathbf{R}$ to be a hard constraint on the n-rank [17] of the tensor $\mathcal{X}$ such that $(\text{rank}(\mathbf{X}_{(1)}), \text{rank}(\mathbf{X}_{(2)}), \text{rank}(\mathbf{X}_{(3)})) \leq (r_1, r_2, r_3)$, where $\mathbf{X}_{(i)}$ denotes the ith order matrix unfolding of tensor $\mathcal{X}$. This hard constraint can be efficiently fulfilled by performing truncated multilinear singular value decomposition (SVD) [18] [19] that reduces the problem size significantly, which is beneficial given the large size of the tensor $\mathcal{X}$.

2.4. Algorithm

We propose an ADMM algorithm to solve this problem efficiently. All subproblems have closed-form solutions. The augmented Lagrangian function can be written as

$$\begin{aligned} L(\mathbf{x}, \mathbf{y}, \mathbf{u}_1, \mathbf{u}_2, \mathcal{X}) = &\|\mathbf{d} - \Omega\mathbf{y}\|_2^2 + \lambda \mathbf{R}(\mathcal{X}) \\ &+ \mu_1(\|\mathbf{y} - \mathcal{F}\mathbf{P}\mathbf{x} + \mathbf{u}_1\|_2^2 - \|\mathbf{u}_1\|_2^2) \\ &+ \mu_2(\|\text{vec}(\mathcal{X} - \mathcal{H}\mathcal{F}\mathbf{P_1}\mathbf{x} + \mathbf{u}_2)\|_2^2 \\ &- \|\text{vec}(\mathbf{u}_2)\|_2^2) \end{aligned} \tag{2}$$

where vec denotes vectorization. We minimize (2) by updating splitting variables iteratively

$$\mathbf{y}^{k+1} = (\Omega^*\Omega + \mu_1\mathbf{I})^{-1}\big(\Omega^*\mathbf{d} + \mu_1(\mathcal{F}\mathbf{P}\mathbf{x}^k - \mathbf{u}_1)\big), \tag{3}$$

by matrix inversion lemma

$$\begin{aligned} (\Omega^*\Omega + \mu_1\mathbf{I})^{-1} &= \frac{\mathbf{I}}{\mu_1} - \frac{1}{\mu_1}\Omega^*(\mathbf{I} + \frac{\Omega\Omega^*}{\mu_1})^{-1}\Omega\frac{1}{\mu_1} \\ &= \frac{1}{\mu_1}\big(\mathbf{I} - \frac{\Omega^*\Omega}{1 + \mu_1}\big), \end{aligned} \tag{4}$$

as $\Omega\Omega^* = \mathbf{I}$. Putting (4) back into (3), after some simplifications, we can show

$$\begin{aligned} \mathbf{y}^{k+1} = &\frac{\Omega^*\mathbf{d} + \mu_1\Omega^*\Omega(\mathcal{F}\mathbf{P}\mathbf{x}^k - \mathbf{u}_1)}{1 + \mu_1} \\ &+ (\mathbf{I} - \Omega^*\Omega)(\mathcal{F}\mathbf{P}\mathbf{x}^k - \mathbf{u}_1), \end{aligned} \tag{5}$$

which can be calculated easily by updating sampled locations of $\mathbf{y}$ using the weighted-average of k-space samples and $(\mathcal{F}\mathbf{P}\mathbf{x}^k - \mathbf{u}_1)$, and unsampled locations using $(\mathcal{F}\mathbf{P}\mathbf{x}^k - \mathbf{u}_1)$. The update of $\mathbf{x}$ is

$$\begin{aligned} \mathbf{x}^{k+1} = \text{Real}\big(&\mu_1\mathbf{P}^*\mathcal{F}^*(\mathbf{y}^{k+1} + \mathbf{u}_1^k) \\ &+ \mu_2\mathbf{P}_1^*\mathcal{F}^*\mathcal{H}^*(\mathcal{X}^k + \mathbf{u}_2^k)\big)/(\mu_1 + \mu_2), \end{aligned} \tag{6}$$

where $\mathcal{H}^*$ is an operator that averages antidiagonal entries in the block-Hankel matrix (which are replicates of the same k-space samples) and puts the average back into appropriate locations [15]. By construction, $\mathcal{H}^*\mathcal{H}$ is an identity operator. The update of the low-rank tensor is calculated as

$$\mathcal{X}^{k+1} = \text{mlsvd}(\mathcal{H}\mathcal{F}\mathbf{P_1}\mathbf{x}^{k+1} - \mathbf{u}_2^k), \tag{7}$$

where mlsvd is the truncated multilinear singular value decomposition, as described in section 2.3, with a core tensor size of (r_1, r_2, r_3). The code is available online [20]. The updates of auxiliary variables are

$$\mathbf{u}_1^{k+1} = \mathbf{u}_1^k + (\mathbf{y}^{k+1} - \mathcal{F}\mathbf{P}\mathbf{x}^{k+1}) \tag{8}$$

$$\mathbf{u}_2^{k+1} = \mathbf{u}_2^k + (\mathcal{X}^{k+1} - \mathcal{H}\mathcal{F}\mathbf{P_1}\mathbf{x}^{k+1}) \tag{9}$$

3. METHOD

3.1. Data preparation

Under IRB approval, a patient was scanned with a DW EPI sequence on a Siemens 3T scanner with a 20-channel coil array and 3 orthogonal diffusion directions. Eleven b-values were sampled uniformly from 0 s/mm^2 to 2500 s/mm^2, with TR = 9300 ms, TE = 93 ms and flip angle = 90°. To ensure a reasonable geometric fidelity, four-fold parallel imaging (GRAPPA) [14] and partial Fourier [16] (with 75% of k-space sampled) were applied during data acquisition.

We also simulated a DWI dataset, using a brain phantom from brainweb [21] and imaging parameters the same as the patient scan. We removed the skull and simulated diffusion signals for white matter, gray matter and fluid using a bi-exponential decay model [22]. We estimated coil phase maps from the patient dataset and simulated phase variations across b-values assuming rigid body motion and linear phase variations [23]. We added Gaussian white noise to the simulated k-space data, with noise covariance matrix estimated from the noise calibration lines of the patient scan.

3.2. k-space sampling and phase map estimation

We retrospectively undersampled the k-space of both datasets, where we fully sampled the center of the k-space, and randomly undersampled the peripheral part of k-space, along the phase-encoding direction only. Note that the patient dataset was undersampled by 4 with a quarter plane of k-space not acquired. Our sampling scheme further undersamples this dataset. We undersampled the simulated dataset the same way as the patient dataset. Both undersamplings of patient and simulated dataset achieve an acceleration factor of 8.0, defined as the ratio between the full data size and sampled data size. We repeated the random sampling process to test the stability of our algorithm. Figure 1 shows example sampling scheme of patient data.

We estimated the phase map at each coil/b-value by first calculating a GRAPPA [14] kernel from the auto-calibration region at $b = 0$ s/mm^2 and filling up the regularly undersampled k-space center for other b-values. The phase map was then calculated from the GRAPPA-filled center of k-space.

3.3. Evaluation

We compared our method with two other low-rank model-based methods: the phase-constrained low-rank matrix model [7] (denoted as the PCLR method) and the low-rank tensor model with coil as one dimension [12] (denoted as the LRT method).

For the simulated dataset, we quantitatively evaluated our reconstruction error by comparing our results $\hat{\gamma}$ to the noise-free groundtruth γ. We calculated the reconstruction error as

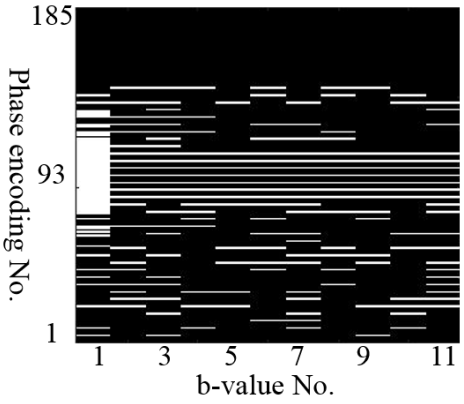

Fig. 1: Sampling scheme of patient data. White lines indicate sampled readouts.

$\|\gamma - \hat{\gamma}\|_2 / \|\gamma\|_2$. For the patient dataset, due to the poor signal-to-noise ratio at high b-values, which is further degraded by parallel imaging, the reconstruction difference between our results and the one by parallel imaging is not informative. Instead, we evaluated the SNR of the reconstructed images using different methods.Characterization of noise distributions in reconstructed MR images has been an open problem [24]. We chose the standard definition of SNR in imaging (ratio between mean signal of the imaging object and standard deviation of the background) for simplicity, while more sophisticated noise characterization schemes may be used in future work.

4. RESULT

Figure 2 shows the reconstruction results using (1) parallel imaging (PI) using GRAPPA [14]; (2) PCLR [7]; (3) LRT [12]; and (4) our proposed method. All methods perform well at $b = 0$ s/mm^2, possibly due to the high SNR and the fully sampled auto-calibration region. However, at a high b-value ($b = 2500$ s/mm^2), PI and PCLR result in poor SNR and the LRT method shows aliasing (indicated by the red arrow), while our method still produces clean reconstruction.

Figure 3 shows the reconstruction results using the simulated dataset at $b = 2500$ s/mm^2, as well as the absolute difference maps as compared to the noise-free groundtruth. The reconstruction by PCLR is blurry while the reconstruction by LRT shows aliasing, as can be visualized from the difference map. Although the aliasing is not strongly visible in the image, it may affect subsequent image analysis using higher-order diffusion models such as the bi-exponential model [22], as the non-linear fitting procedure is very sensitive to errors. Repeating the experiment with another random sampling scheme shows similar results. The overall reconstruction error for 4-fold PI is 10.0%, and 14.0%/17.8%, 6.4%/11.7%, 3.6%/4.3% respectively for the two repeated ex-

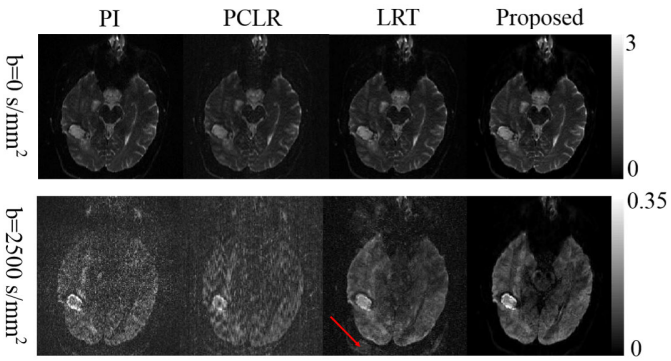

Fig. 2: Reconstruction results using patient data.

periments using PLCR, LRT and our proposed method.

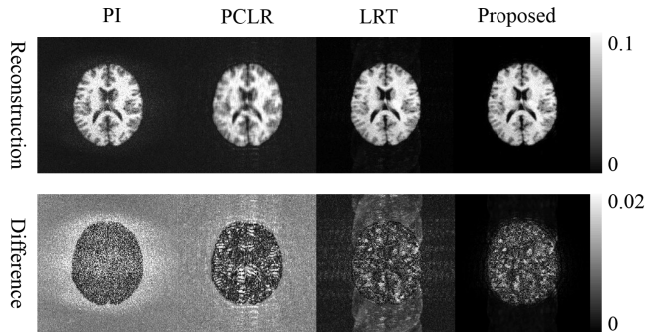

Fig. 3: Reconstruction results using simulated data at b=2500 s/mm^2.

Figure 4 compares different methods by plotting the SNR of reconstructed images at different b-values using patient data and reconstruction errors (averaged between 2 repeated experiments) at different b-values using simulated data. Our method consistently achieves superior SNR and lower reconstruction error for all b-values.

5. CONCLUSION AND DISCUSSION

In this work we develop a low-rank tensor model with phase constraint, to accelerate the acquisition of high b-value DWI for cancer imaging. Our model exploits both the local and global low-rank structure of the DWI data. The problem formulation integrates parallel imaging and partial Fourier reconstruction, two commonly used acceleration schemes in clinic. The reconstruction results, with an acceleration factor of 8, show improved SNR and reduced aliasing as compared to other image reconstruction methods.

One important parameter in low-rank models is the rank number. Currently it is decided by visually inspecting the singular value distributions of unfolding matrices. Future work will evaluate the selection of rank constraint more systematically. Future work will also estimate diffusion parameters from our reconstruction results, using higher-order diffusion models [1] [22] rather than mono-exponential decay models, to extract potential new biomarkers for tumor delineation, grading and treatment response assessment.

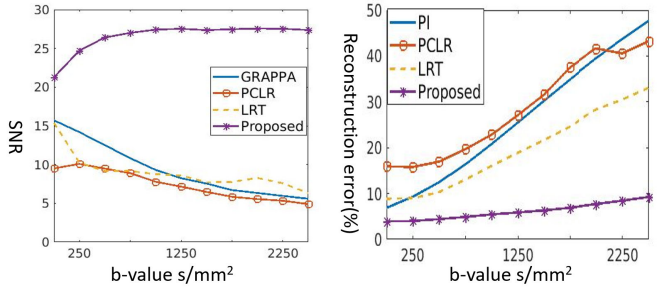

Fig. 4: Left: SNR of reconstructed images using patient data; right: reconstruction errors using simulated data.

6. ACKNOWLEDGEMENT

This work is supported by NIHR01EB016079 and Rackham Barbour Scholarship.

7. REFERENCES

[1] T.C. Kwee, C.J. Galbán, C. Tsien, L. Junck, P.C. Sundgren, M.K. Ivancevic, T.D. Johnson, C.R. Meyer, A. Rehemtulla, and B.D. Ross, "Comparison of apparent diffusion coefficients and distributed diffusion coefficients in high-grade gliomas," *Journal of Magnetic Resonance Imaging*, vol. 31, no. 3, pp. 531–537, 2010.

[2] B.A. Hoff, T.L. Chenevert, M.S. Bhojani, T.C. Kwee, A. Rehemtulla, D. Le Bihan, B.D. Ross, and C.J. Galbán, "Assessment of multiexponential diffusion features as MRI cancer therapy response metrics," *Magnetic resonance in medicine*, vol. 64, no. 5, pp. 1499–1509, 2010.

[3] P.P. Pramanik, H.A. Parmar, A.G. Mammoser, L.R. Junck, M.M. Kim, C. Tsien, T.S. Lawrence, and Y. Cao, "Hypercellularity components of glioblastoma identified by high b-value diffusion-weighted imaging," *International Journal of Radiation Oncology Biology Physics*, vol. 92, no. 4, pp. 811–819, 2015.

[4] C. Liao, Y. Chen, X. Cao, S. Chen, H. He, M. Mani, M. Jacob, V. Magnotta, and J. Zhong, "Efficient parallel reconstruction for high resolution multishot spiral diffusion data with low rank constraint," *Magnetic resonance in medicine*, vol. 77, no. 3, pp. 1359–1366, 2017.

[5] M. Mani, M. Jacob, A. Guidon, V. Magnotta, and J. Zhong, "Acceleration of high angular and spatial resolution diffusion imaging using compressed sensing with multichannel spiral data," *Magnetic resonance in medicine*, vol. 73, no. 1, pp. 126–138, 2015.

[6] J.P. Haldar and K. Setsompop, "Fast high-resolution diffusion MRI using gSlider-SMS, interlaced subsampling, and SNR-enhancing joint reconstruction," in *Proceedings of the 25th Annual Meeting of ISMRM, Honolulu, HI, USA*, 2017.

[7] H. Gao, L. Li, K. Zhang, W. Zhou, and X. Hu, "PCLR: Phase-constrained low-rank model for compressive diffusion-weighted MRI," *Magnetic resonance in medicine*, vol. 72, no. 5, pp. 1330–1341, 2014.

[8] X. Shi, X. Ma, W. Wu, F. Huang, C. Yuan, and H. Guo, "Parallel imaging and compressed sensing combined framework for accelerating high-resolution diffusion tensor imaging using inter-image correlation," *Magnetic resonance in medicine*, vol. 73, no. 5, pp. 1775–1785, 2015.

[9] S.F. Roohi, D. Zonoobi, A.A. Kassimand, and J.L. Jaremko, "Dynamic MRI reconstruction using low rank plus sparse tensor decomposition," in *Proc. ICIP*. IEEE, 2016, pp. 1769–1773.

[10] D. Banco, S. Aeron, and W.S. Hoge, "Sampling and recovery of MRI data using low rank tensor models," in *Proc. EMBC*. IEEE, 2016, pp. 448–452.

[11] J. He, Q. Liu, A.G. Christodoulou, C. Ma, F. Lam, and Z. Liang, "Accelerated high-dimensional MR imaging with sparse sampling using low-rank tensors," *IEEE transactions on medical imaging*, vol. 35, no. 9, pp. 2119–2129, 2016.

[12] J.D. Trzasko and A. Manduca, "A unified tensor regression framework for calibrationless dynamic, multichannel MRI reconstruction," in *Proceedings of the 21st Annual Meeting of ISMRM, Salt Lake City, Utah, USA*, 2013, p. 603.

[13] Y. Liu, J. Cao, M. Lyu, and E.W. Wu, "Calibrationless parallel imaging reconstruction using hankel tensor completion (htc)," in *Proceedings of the 25th Annual Meeting of ISMRM, Honolulu, HI, USA*, 2017.

[14] M.A. Griswold, P.M. Jakob, R.M. Heidemann, M. Nittka, V. Jellus, J. Wang, B. Kiefer, and A. Haase, "Generalized autocalibrating partially parallel acquisitions (GRAPPA)," *Magnetic resonance in medicine*, vol. 47, no. 6, pp. 1202–1210, 2002.

[15] P.J. Shin, P.E. Larson, M.A. Ohliger, M. Elad, J.M. Pauly, D.B. Vigneron, and M. Lustig, "Calibrationless parallel imaging reconstruction based on structured low-rank matrix completion," *Magnetic resonance in medicine*, vol. 72, no. 4, pp. 959–970, 2014.

[16] E.M. Haacke, E.D. Lindskogj, and W. Lin, "A fast, iterative, partial-Fourier technique capable of local phase recovery," *Journal of Magnetic Resonance*, vol. 92, no. 1, pp. 126–145, 1991.

[17] L. De Lathauwer, B. De Moor, and J. Vandewalle, "A multilinear singular value decomposition," *SIAM journal on Matrix Analysis and Applications*, vol. 21, no. 4, pp. 1253–1278, 2000.

[18] N. Vannieuwenhoven, R. Vandebril, and K. Meerbergen, "A new truncation strategy for the higher-order singular value decomposition," *SIAM Journal on Scientific Computing*, vol. 34, no. 2, pp. A1027–A1052, 2012.

[19] N. Halko, P. Martinsson, and J.A. Tropp, "Finding structure with randomness: Probabilistic algorithms for constructing approximate matrix decompositions," *SIAM review*, vol. 53, no. 2, pp. 217–288, 2011.

[20] N. Vervliet, O. Debals, L. Sorber, M. Van Barel, and L. De Lathauwer, "Tensorlab 3.0," Mar. 2016, Available online.

[21] D.L. Collins, A.P. Zijdenbos, V. Kollokian, J.G. Sled, N.J. Kabani, C.J. Holmes, and A.C. Evans, "Design and construction of a realistic digital brain phantom," *IEEE transactions on medical imaging*, vol. 17, no. 3, pp. 463–468, 1998.

[22] R.V. Mulkern, H.P. Zengingonul, R.L. Robertson, P. Bogner, K.H. Zou, H. Gudbjartsson, C.R. Guttmann, D. Holtzman, W. Kyriakos, and F.A. Jolesz, "Multicomponent apparent diffusion coefficients in human brain: relationship to spin-lattice relaxation," *Magnetic resonance in medicine*, vol. 44, no. 2, pp. 292–300, 2000.

[23] A.T. Van, D.C. Karampinos, J.G. Georgiadis, and B.P. Sutton, "k-space and image space combination for motion artifact correction in multicoil multishot diffusion weighted imaging," in *Proc. EMBC*. IEEE, 2008, pp. 1675–1678.

[24] O. Dietrich, J.G. Raya, S.B. Reeder, M.F. Reiser, and S.O. Schoenberg, "Measurement of signal-to-noise ratios in MR images: Influence of multichannel coils, parallel imaging, and reconstruction filters," *Journal of Magnetic Resonance Imaging*, vol. 26, no. 2, pp. 375–385, 2007.